INT. J. NUM. METH. HEAT FLUID FLOW, VOL. 3, 157–172 (1993)

APPLICATION OF THE HOMOGRAPHIC APPROXIMATION IN THE ENTHALPY METHOD FOR PHASE CHANGE PROBLEMS

MINWU YAO

Ohio Aerospace Institute, 22800 Cedar Point Road, Book Park, Ohio 44142, USA

AND

ARNON CHAIT

NASA Lewis Research Center, MS 105-1, Cleveland, OH 44135, USA

ABSTRACT

The homographic approximation, in which the Heaviside step function is replaced by a continuous smooth curve, is applied to the enthalpy method for heat transfer problems with isothermal phase change. Both the finite difference and finite element implementations, based on the basic enthalpy, the apparent heat capacity and the source term formulations, are considered. A 1-D Stefan problem of melting a solid is used as a test problem. The accuracy of the numerical solutions is measured globally using L_2 error norms and comparison is made between the solutions using homographic approximation and those using linear approximation. The advantages of using homographic approximation are examined.

KEYWORDS Homographic approximation Enthalpy method Stefan problem Phase change Finite difference method Finite element method

INTRODUCTION

The modelling of liquid/solid phase change problems is important in many areas of science and engineering. Because experimental analysis is often prohibitively expensive and analytical solutions are generally unavailable for most of the practical problems, the motivation for numerical simulation is obvious and various mathematical/computational techniques have been developed in this field during recent years[1–11].

In the numerical modelling of heat transport with phase change, the so-called enthalpy method[1] has become a popular tool due to its important features, such as the ease of implementation in existing heat transfer programs, no computational overheads associated with tracking the moving interface, and validity for multi-dimensional problems with complicated interface shapes, etc. In the enthalpy formulation, the latent heat evolution condition on the moving interface is incorporated into the governing energy equation by introducing either a total enthalpy function, a modified specific heat coefficient, or a heat source term. Consequently the interface tracking and mesh deforming can be avoided and the numerical solution can be carried out on a fixed space grid.

For isothermal phase change (i.e. at a single temperature), the enthalpy function, $H(T)$, or equivalently the liquid volume fraction function[7], $g(T)$, introduced in the enthalpy formulation,

0961–5539/93/020157–16$2.00

Received May 1992
Revised September 1992

is discontinuous across the liquid/solid interface. The jump of $H(T)$ at the melting temperature is equal to the latent heat. It is this discontinuity of $H(T)$ that renders great difficulties in numerical solutions of phase change problems. A natural way to improve the discontinuity of the enthalpy function is to approximate the $H-T$ curve by smoothed functions and solve the problem on the basis of weak formulation[1,12–14]. The smoothing schemes for $H(T)$ currently used in the literature are usually C^0 continuous (with discontinuous derivative). Consequently the numerical solutions based on these C^0 smoothing schemes have the following undesired properties:

(i) the definition of the approximated $H(T)$ is usually piecewise, which involves multiple temperature intervals,
(ii) the numerical formulations are usually different on these temperature intervals, which makes the numerical algorithm and implementation complicated,
(iii) the accuracy of temperature gradient in the vicinity of the liquid/solid interface is usually unsatisfactory due to the C^0 approximation,
(iv) it is well documented in the literature[1,2,15–17] that the conventional discretizations of the enthalpy method have a tendency to oscillate numerically in temperature and phase front position. This is caused by over-looking the discontinuous behaviour of temperature gradient and enthalpy at the interface.

An idea to overcome these defects is to introduce a differentiable approximation for $H(T)$, i.e. the so-called homographic approximation. This approximation, in conjunction with the freezing index[1], has been employed by Brauner *et al.*[18] in a parabolic variational inequality formulation of the multiphase Stefan problems. Blanchard and Fremond used[19] the homographic approximation to approximate the specific energy function in a variational equality formulation for the free boundary problems.

In this paper we use the homographic approximation to approximate the enthalpy function in the enthalpy formulation based on the differential heat transport equation for phase change problems and examine the advantages. Both the finite different method (FDM) and the finite element method (FEM) implementations, including the associated discretization and solution schemes, are studied through three representative enthalpy formulations. A classical 1-D Stefan problem is used as a test problem and some promising and interesting numerical observations are reported.

MATHEMATICAL MODEL

For simplicity of presentation, consider the classical 1-D Stefan problem for phase changes in a pure substance in which the phase transition is governed by the equation of heat transport only. The mathematical model[1,20] consists of the following parabolic differential equation:

$$\rho_i c_i \frac{\partial T_i}{\partial t} = \frac{\partial}{\partial x}\left(\kappa_i \frac{\partial T_i}{\partial x}\right) \qquad \forall (x,t) \in \Omega_i \times [0,\tau] \tag{1}$$

coupled with appropriate initial conditions, boundary conditions, and the following liquid/solid interface conditions:

$$T_s[S(t),t] = T_l[S(t),t] = T_m \tag{2}$$

$$\kappa_s \frac{\partial T_s}{\partial x} - \kappa_l \frac{\partial T_l}{\partial x} = \rho L \frac{\mathrm{d}S}{\mathrm{d}t} \tag{3}$$

Here subscripts $i = s, l$ denote solid phase and liquid phase; $\Omega = \Omega_s \cup \Omega_l$ is the domain of interest; ρ_i, c_i, κ_i, T_i are density, specific heat, heat conductivity and temperature for phase i; t is time; $S(t)$ is the position of interface; L is the latent heat; T_m is the melting temperature.

ENTHALPY FORMULATIONS AND NUMERICAL SCHEMES

In order to test homographic approximation, we consider the following three typical enthalpy formulations.

Basic enthalpy formulation (BEF)

On neglecting convection effects, the basic enthalpy formulation for a conduction controlled phase change is given by:

$$\frac{\partial H}{\partial t} = \frac{\partial}{\partial x}\left(\kappa \frac{\partial T}{\partial x}\right) \qquad \forall (x, t) \in \Omega \times [0, \tau] \tag{4}$$

where H is the enthalpy function defined as[1,21]:

$$H(T, g) = \int_{T_{ref}}^{T} \rho c \, \mathrm{d}\theta + \rho g(T) L \tag{5}$$

Here T_{ref} is an arbitrary reference temperature and g is the local liquid volume fraction[7,21]. For an isothermal phase change, g is given by the Heaviside step function:

$$g(T) = \begin{cases} 0, & T < T_m \\ 1, & T > T_m \end{cases} \tag{6}$$

Standard FDM schemes. Applying the standard FDM discretization and the θ-method to (4) gives the following well-known schemes[11] in point form:

$$H(T_i^{k+1}) - \theta\lambda\kappa(T_{i-1}^{k+1} - 2T_i^{k+1} + T_{i+1}^{k+1}) = H(T_i^k) + (1-\theta)\lambda\kappa(T_{i-1}^k - 2T_i^k + T_{i+1}^k) \tag{7}$$

where $\lambda = \Delta t/(\Delta x)^2$, $T_i^k = T(i\Delta x, k\Delta t)$ and $0 \leqslant \theta \leqslant 1$.

Standard FEM schemes. Based on Galerkin's formulation and the standard FEM discretization using linear element, the point form FEM schemes for (4) can be written as[11,22]:

$$\begin{aligned} &[H(T_{i-1}^{k+1}) + 4H(T_i^{k+1}) + H(T_{i-1}^{k+1})]/6 - \theta\lambda\kappa(T_{i-1}^{k+1} - 2T_i^{k+1} + T_{i+1}^{k+1}) \\ &= [H(T_{i-1}^k) + 4H(T_i^k) + H(T_{i+1}^k)]/6 + (1-\theta)\lambda\kappa(T_{i-1}^k - 2T_i^k + T_{i+1}^k) \end{aligned} \tag{8}$$

where the definitions of λ and θ are the same as that in (7). Equation (8) is usually referred to as consistent (or distributed) capacitance formulation. It has been shown in the literature[23,24] that the use of lumped capacitance in the FEM solution of phase change problems has some advantages over the consistent treatment. For 1-D problems, it is easy to prove that the FEM formulation with lumped capacitance is identical with the FDM formulation (7).

Note that in this paper we treat (7) and (8) as T-version formulations in which temperature is the primary variable and the enthalpy is computed from the definition of (5) or some other smoothed functions that will be presented later.

Apparent heat capacity (AHC) formulation

From (5) an apparent heat capacity can be defined as:

$$C^A(T) \equiv \frac{\mathrm{d}H}{\mathrm{d}T} = \rho c + \rho L \frac{\mathrm{d}g}{\mathrm{d}T} \tag{9}$$

By using the definition of AHC, (4) can be rewritten as:

$$C^A(T)\frac{\partial T}{\partial t} = \frac{\partial}{\partial x}\left(\kappa\frac{\partial T}{\partial x}\right) \tag{10}$$

which is often called as apparent (or modified) heat capacity formulation[4,25,26].

For both the FDM and FEM cases, discretization of (10) leads to the following system in matrix form:

$$\left[\frac{1}{\Delta t}\mathbf{C}(\mathbf{T}^*) + \theta\mathbf{K}(\mathbf{T}^{k+1})\right]\mathbf{T}^{k+1} = \left[\frac{1}{\Delta t}\mathbf{C}(\mathbf{T}^*) + (\theta - 1)\mathbf{K}(\mathbf{T}^k)\right]\mathbf{T}^k \tag{11}$$

where $\mathbf{T}^k$ is the temperature vector; $\mathbf{K}(\mathbf{T})$ is the conductance matrix; and the $\mathbf{C}(\mathbf{T}^*)$ is the capacitance matrix. For the AHC formulation, the numerical evaluation of $\mathbf{C}(\mathbf{T}^*)$ is of crucial importance. In this paper we shall treat $\mathbf{C}(\mathbf{T}^*)$ explicitly by letting $\mathbf{T}^* = \mathbf{T}^k$ and use the post-iteration correction scheme proposed by Pham[23] and Comini *et al.*[27]. This correction scheme consists of two steps for each iteration. First, (11) serves as a predictor. Then, the following corrector is used to calculate the corrected temperature:

$$\tilde{\mathbf{T}}^{k+1} = E(\mathbf{H}^{k+1}) \tag{12}$$

where E is the inverse of H and $\mathbf{H}^{k+1}$ is the corrected enthalpy value by:

$$\mathbf{H}^{k+1} = \mathbf{H}^k + \mathbf{C}(\mathbf{T}^k)(\mathbf{T}^{k+1} - \mathbf{T}^k) \tag{13}$$

Source term formulation (STF)[10,21]

An alternative to incorporating the latent heat into the enthalpy function is to treat the latent heat as a source term in the governing equation. Following Voller[21], we split the total enthalpy into sensible and latent heat components, namely

$$H(T) = h(T) + \rho g L \tag{14}$$

where

$$h(T) = \int_{T_{ref}}^{T} \rho c \, \mathrm{d}\theta \tag{15}$$

Assuming ρ, c = constant, substitution of (14) into (4) yields the following source term formulation:

$$\frac{\partial h}{\partial t} = \frac{\partial}{\partial x}\left(\frac{\kappa}{\rho c}\frac{\partial h}{\partial x}\right) - \rho L\frac{\partial g}{\partial t} \tag{16}$$

in which $-\rho L\partial g/\partial t$ is isolated as a non-linear source term. The standard FDM schemes and the equivalent lumped-capacitance FEM schemes are given by:

$$\begin{aligned} &h_i^{k+1} - \theta\lambda\kappa(h_{i-1}^{k+1} - 2h_i^{k+1} + h_{i+1}^{k+1}) \\ &= h_i^k + (1-\theta)\lambda\kappa(h_{i-1}^k - 2h_i^k + h_{i+1}^k) - \rho L[g_i^{k+1} - g_i^k] \end{aligned} \tag{17}$$

Here we treat (17) as an h-version formulation. A fast iterative solution procedure based on STF was proposed by Voller[21].

APPROXIMATIONS FOR ENTHALPY FUNCTION

An important fact pertaining to the enthalpy formulation for isothermal phase change problems is that the derivative, $\partial H/\partial t$ in (4), is not well defined in the classical sense at $T = T_m$, due to the discontinuity of $H(T)$. In practice, the generalized solutions to the original (4) are usually obtained as the limit of a uniformly convergent sequence of classical solutions to approximating problems, deduced by smoothing the $H(T)$ curve and the coefficient in (4). It has been known that the smoothing scheme employed for approximating the enthalpy function, or equivalently the liquid fraction function, is of prime importance to the success of the enthalpy method.

Linear approximation

The simplest and most popular smoothing scheme for $H(T)$ is perhaps the following linear approximation:

$$H(T) \approx H_\varepsilon(T) \equiv H(T, g_\varepsilon) \tag{18}$$

obtained by replacing g in (5) with g_ε which is a linear approximation for the Heaviside step function defined as:

$$g_\varepsilon(T) \equiv \begin{cases} 0 & T \leqslant T_m - \varepsilon \\ \dfrac{1}{2\varepsilon}[T - (T_m - \varepsilon)] & T_m - \varepsilon < T < T_m + \varepsilon \\ 1 & T \geqslant T_m + \varepsilon \end{cases} \tag{19}$$

where ε is the semi-length of the mushy zone. On substituting (19) into (5) and assuming ρ_i, c_i are constants leads to an explicit expression for (18), viz.

$$H_\varepsilon(T) \equiv \begin{cases} \rho_s c_s T & T < T_m - \varepsilon \\ \rho_s c_s (T_m - \varepsilon) + \left(\dfrac{\rho_s c_s + \rho_l c_l}{2} + \dfrac{\rho_s L}{2\varepsilon}\right)[T - (T_m - \varepsilon)] & T_m - \varepsilon < T < T_m + \varepsilon \\ \rho_s c_s T_m + \rho_l c_l (T - T_m) + \rho_s L & T > T_m + \varepsilon \end{cases} \tag{20}$$

For AHC formulation, (20) corresponds to approximating the AHC (9) by the following step function used by Bonacina *et al.*[28]:

$$C^A \approx C^A_\varepsilon(T) = \begin{cases} \rho_s c_s & T < T_m - \varepsilon \\ \dfrac{\rho_s c_s + \rho_l c_l}{2} + \dfrac{\rho_s L}{2\varepsilon} & T_m - \varepsilon < T < T_m + \varepsilon \\ \rho_l c_l & T > T_m + \varepsilon \end{cases} \tag{21}$$

It is easy to see that approximation (20) is C^0-continuous only.

Homographic approximation

To improve the smoothness of the approximated $H(T)$ curve, we introduce the so-called homographic approximation for the Heaviside step function, that is:

$$g(T) \approx g_\eta(T) \equiv \frac{1}{2}\left(\frac{T - T_m}{\eta + |T - T_m|} + 1\right) \tag{22}$$

This approximation, based on the properties of the homographic mapping is directly inspired from the singular limits of reaction diffusion equations modelling heterogeneous chemical catalyst and enzyme kinetics with absorption[29-31].

The great advantage of homographic approximation is its differentiability. As a matter of fact, $g_\eta(T)$ is C^1-continuous in T. By differentiating (22) with respect to T, we have:

$$g'_\eta = \frac{dg_\eta}{dT} = \frac{1}{2\eta(1 + |T - T_m|/\eta)^2} \tag{23}$$

which is continuous for all T. The definition of g_η involves a parameter η, which is analogous to the ε in the linear approximation. The effect of η on the shapes of $g_\eta(T)$ and its derivative is illustrated schematically in *Figure 1*. By decreasing the value of η, the error of homographic approximation can be reduced monotonically. Theoretically speaking the homographic approximation curve can be used to approach the jump discontinuity infinitely by controlling the parameter η while still maintaining its C^1 continuity.

Now we can define a smoothed enthalpy curve in terms of the homographic approximation as:

$$H(T) \approx H_\eta(T) \equiv H(T, g_\eta) \tag{24}$$

where g_η is given by (22). In the limit we shall have:

$$\lim_{\eta \to 0} H_\eta(T) = H(T) \tag{25}$$

As an example, consider a special case where ρ_i, c_i are constants and the same in both liquid and solid phases, i.e. $\rho_s = \rho_l = \rho$, $c_s = c_l = c$. In this case (24) can be expressed explicitly as:

$$H_\eta(T) = \rho c(T - T_m) + \frac{\rho L}{2}\left(\frac{T - T_m}{\eta + |T - T_m|} + 1\right) \tag{26}$$

Based on (26) the corresponding AHC is given by:

$$C^A \approx C^A_\eta(T) = \rho c + \frac{\rho L}{2\eta}\frac{1}{(1 + |T - T_m|/\eta)^2} \tag{27}$$

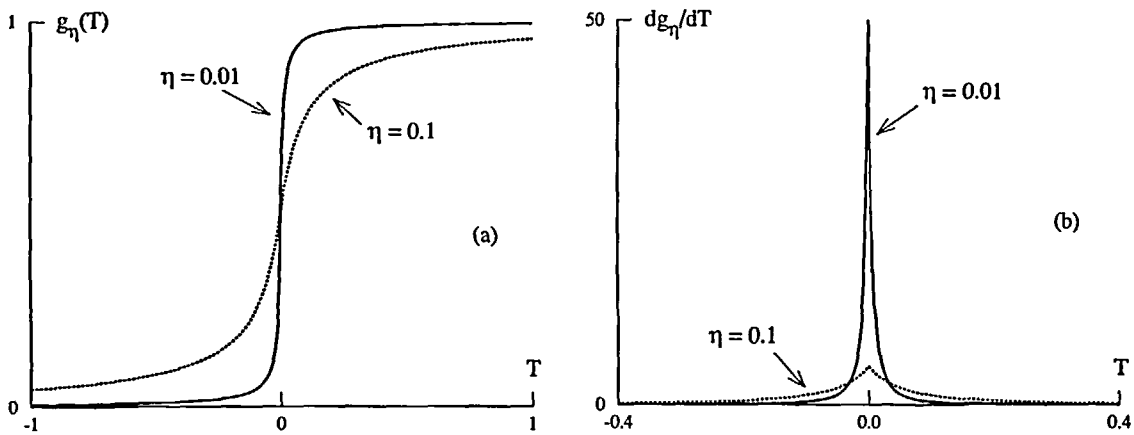

Figure 1 The homographic approximation for the local liquid volume fraction, $g_\eta(T)$ given by (22) and its derivative dg_η/dT (23), at two different values of η

For convenience and without losing generality, we shall assume $T_m = 0$ and hence $T - T_m$ in (26), (27) can be replaced by T.

Implementing the homographic approximation in FDM

In the linear approximation (20), $H_\varepsilon(T)$ is defined piecewise in three intervals and the expressions for FDM or FEM schemes on these intervals are different. In the homographic approximation, however, the definitions (26) and (27) are valid on the whole domain. This makes the implementation work much easier. To illustrate how the homographic approximation is implemented in the standard FDM and FEM schemes, we take the T-version BEF (3) as an example and consider the standard 1-D FDM schemes given by (7). The non-linear Gauss–Seidel SOR algorithm[11] can be written as follows:

$$\tilde{T}_i^{k+1} = R^{-1}[\underbrace{f_i^k + \theta\lambda\kappa(T_{i-1}^{k+1} + T_{i+1}^k)}_{d_i^k}] \tag{28}$$

$$T_i^{k+1} = (1 - w)T_i^k + w\tilde{T}_i^{k+1} \tag{29}$$

where $1 \leqslant w < 2$ is the over relaxation factor and

$$f_i^k = H_\eta(T_i^k) + (1 - \theta)\lambda\kappa(T_{i-1}^k - 2T_i^k + T_{i+1}^k) \tag{30}$$

To proceed with the iteration algorithm (28), we need to compute an inverse function R^{-1}. For homographic approximation, by substituting (22) into (7), collecting the T_i^{k+1} terms and assuming $T_m = 0$, $c_s = c_l = c$, we obtain the function $R(T)$ in the following form:

$$R(T) = \frac{\rho L}{2}\left(\frac{T}{\eta + |T|} + 1\right) + (\rho c + 2\theta\lambda\kappa)T = d_i^k \tag{31a}$$

Let $b_i = \rho c + 2\theta\lambda\kappa$; then (31a) can be rewritten as:

$$b_i T|T| + (\rho L/2 + b_i\eta)T + (\rho L/2 - d_i^k)|T| + (\rho L/2 - d_i^k)\eta = 0 \tag{32}$$

In order to solve this quadratic equation, we need to know the sign information of T on the basis of d_i^k and other known parameters. This is actually fairly easy if we rewrite (31a) in the following form:

$$\left(b_i + \frac{\rho L}{2}\frac{1}{\eta + |T|}\right)T = d_i^k - \frac{\rho L}{2} \tag{31b}$$

and noting the fact that:

$$b_i + \frac{\rho L}{2}\frac{1}{\eta + |T|} > 0 \tag{33}$$

Equations (31) and (33) suggest the following relation:

$$\text{sign}(T) = \text{sign}(d_i^k - \rho L/2) \tag{34}$$

By using (34) we rewrite (32) into two separate quadratic equations, namely

$$\begin{cases} b_i T^2 + (\rho L + b_i\eta - d_i^k)T + (\rho L/2 - d_i^k)\eta = 0, & d_i^k \geqslant \rho L/2 \\ b_i|T|^2 + (b_i\eta + d_i^k)|T| - (\rho L/2 - d_i^k)\eta = 0 & d_i^k < \rho L/2 \end{cases} \tag{35}$$

where the first equation is for $T \geqslant 0$ and the second corresponds to $T < 0$. So far the inversion of $R(T)$ has been reduced to the solution of a quadratic equation given in (35) and this can be done analytically.

It is worth noting that in the linear approximation computation of R^{-1} and $H_\varepsilon(T)$ has to be programmed separately on each of the three temperature intervals. For homographic approximation, however, the formulation presented in this subsection is valid over the whole temperature range.

THE TEST PROBLEM AND NUMERICAL COMPUTATION

Stefan problem[32]

Consider the classical 1-D Stefan problem of melting a solid in the half space region $x > 0$. Initially the material is in the solid phase at a constant temperature $T(x, 0) = T_2 < T_m$. At time $t = 0$ the temperature of the surface $x = 0$ is instantaneously raised and maintained at $T(0, t) = T_1 > T_m$. This will cause a layer of solid to be melted and this melted layer will expand into the solid as time advances. Assuming the heat transfer is diffusion-controlled, this phase change problem is described by the governing equations (1)–(3) with the appropriate initial and boundary conditions. The similarity solution of this 1-D Stefan problem is well known and can be found in References 1 and 20. This problem is adopted throughout this work as a test problem together with the following data:

$$T_1 = T(0, t) = 1, \quad T_2 = T(\infty, t) = -1,$$

$$\rho_s = \rho_l = 1, \quad \kappa_s = \kappa_l = 1,$$

$$c_s = c_l = 1, \quad T_m = 0, \quad L = 1$$

Numerical computation

In this paper the test problem is solved by using the 1-D FDM and FEM schemes. Only a finite part of the semi-infinite domain, i.e. [0, 1], is considered. The boundary conditions imposed are of Dirichlet type with a constant temperature $T_1 = 1$ at $x = 0$ and a time dependent function $\varphi(t)$ at $x = 1$ provided by the similarity solution of the Stefan problem. The transient solutions are computed from an initial time $t_0 = 0.2$ to $t = 0.5$. To observe the convergence of numerical solutions, the FDM grids and the FEM meshes are refined by dividing the spatial element size by half each time. The crudest mesh used in this work, i.e. the mesh 1, has an element size $\Delta x_1 = 0.1$. The subsequent meshes are obtained by defining $\Delta x_2 = \Delta x_1/2$ and $\Delta x_3 = \Delta x_1/4$.

For the BEF and AHC formulation, numerical solutions are obtained by using both the linear and the homographic approximation. The non-linear systems resulted from the FDM and FEM schemes are solved by the non-linear Gauss–Seidel SOR iteration, and the iteration termination is controlled by the relative error norm of the nodal temperature.

For the source term formulation, we compute solutions using the unsmoothed $g(T)$ and its homographic approximation $g_\eta(T)$. When $g(T)$ is employed, we use the algorithm (15) and follow the solution procedure proposed by Voller[21], in which the linearized system is solved by the tridiagonal system solver and the iteration convergence is controlled by the error norm of residue. When $g_\eta(T)$ is used, we find that for some cases the iterations based on (15) fail to converge due to the extra non-linearity introduced in the homographic approximation.

Consequently, (15) is modified as follows:

$$b_i h_i^{k+1} + \frac{L}{2c}\frac{h_i^{k+1}}{\eta + |h_i^{k+1}|} = f_i^k - a_i(h_{i-1}^{k+1} + h_{i+1}^k) \tag{36}$$

$$f_i^k = h_i^k + c_i(h_{i-1}^k - 2h_i^k + h_{i+1}^k) + \rho L(g_i^k - 1/2) \tag{37}$$

where

$$a_i = -\theta\lambda\frac{\kappa}{\rho c}, \quad b_i = 1 - 2a_i, \quad c_i = (1-\theta)\lambda\frac{\kappa}{\rho c} \tag{38}$$

System (36) is solved by the non-linear Gauss–Seidel iteration and the formulation is similar to those derived earlier.

In order to examine the advantage of the homographic approximation, calculations using the homographic approximation are compared with those using the linear approximation or the unsmoothed enthalpy function. The comparisons of accuracy and convergence are made in terms of the following global error measurement.

Global error measurement

In our computation the accuracy of the numerical solutions is measured globally against the similarity solution of the test problem. It is known that any measure of the accuracy involves a choice of particular error norms. To measure the global error we define the following L_2 norms:

$$|e_1| \equiv \left(\sum_k \sum_i [T_i^k - T_{\text{exact}}(x_i, t_k)]^2 \Delta x_i \Delta t_k\right)^{1/2} \tag{39}$$

$$|e_2| \equiv \left(\sum_k \sum_i [Q_{i+1/2}^k - Q_{\text{exact}}(x_{i+1/2}, t_k)]^2 \Delta x_i \Delta t_k\right)^{1/2} \tag{40}$$

$$|e_s| \equiv \left(\sum_k \int_{t_{k-1}}^{t_k} [S(\tau) - S_{\text{exact}}(\tau)]^2 \, d\tau\right)^{1/2} \tag{41}$$

for solutions of temperature, heat flux and interface position, respectively. Here T_i^k is the numerical solution of temperature at grid point x_i and time t_k; $Q_{i+1/2}^k$ is the numerical solution of heat flux at the middle point of element, $x_{i+1/2} = (x_i + x_{i+1})/2$ and at time t_k. Note that $|e_1|$, $|e_2|$ are actually the discrete L_2 norms based on nodal values.

NUMERICAL OBSERVATIONS

For explicit time integration schemes, the time steps usually need to be very small due to the stability condition. Consequently, the smoothness of the $H(T)$ curve is not so important and the homographic approximation may not give much advantage. However, for implicit schemes, especially with large time steps, the advantage of homographic approximation becomes much more distinct. Therefore in the following discussion we shall focus on the implicit schemes only.

Basic enthalpy formulation

It can be seen from (19) and (20) that the linear approximation requires a selected value for parameter ε whose physical meaning is the semi-length of the mushy zone. It has been reported in the literature[2,33–35] that the choice of the value of ε is of considerable importance for the

enthalpy method. To study the effect of parameters ε and η, a typical plot of BEF solutions is given in *Figure 2*, in which the error norm $|e_1|$ of the FDM (or equivalently the lumped-capacitance FEM) solutions of the test problem using the backward scheme (7) are shown for a set of ε and η values ranging from 2.5×10^{-5} to 0.4. For linear approximation, the error measurement presented in *Figure 2* indicates that there exists an optimum ε (where the best accuracy may be obtained) for each particular spatial and time discretization. This optimum ε varies with different meshes. The choice of ε is so significant that by choosing the optimum ε (or its approximation) the accuracy of the numerical solutions can be greatly improved. However, the most dramatic improvement of accuracy happens only within a narrow range of ε-value in the vicinity of the optimum ε, as shown in *Figure 2*. Since the analytical prediction for the optimum ε is generally unavailable, this narrow range needs to be determined through numerical experiment.

In homographic approximation, the parameter η plays a role similar to that of ε in the linear approximation. The results in *Figure 2* also suggest the existence of an optimum η in homographic approximation for each particular mesh. For a wide range of η-value (e.g. $\eta \leqslant 0.4$ for mesh 1 and $\eta \leqslant 0.1$ for mesh 2 as shown in *Figure 2*) the homographic approximation is able to produce better accuracy than the linear approximation in terms of the global error norms. It is interesting to note that when $\varepsilon, \eta \to 0$ the accuracy of the two approximations becomes the same. This is consistent with the theory, because when $\varepsilon, \eta \to 0$ both the linear approximation $g_\varepsilon(T)$ and the homographic approximation $g_\eta(T)$ approach to the same limit, i.e. the unsmoothed step function (6).

Next we consider the consistent-capacitance FEM formulation given by (8). The main difference between (8) and (7) lies that in (8) the averaged value:

$$[H(T_{i-1}) + 4H(T_i) + H(T_{i+1})]/6 \tag{42}$$

which involves two neighbouring elements and 3 nodes is used to approximate $H(T_i)$ in contrast to the direct use of the lumped nodal value $H(T_i)$ in (7). Therefore it is expected that the consistent-capacitance FEM formulation should be more sensitive to the smoothness of the enthalpy function than the lumped-capacitance FEM or FDM would. As an example, the consistent FEM solutions of the test problem are computed using linear and homographic approximations and the Crank–Nicholson scheme. In *Figure 3*, we plot the error norms of these solutions. A big difference between the results shown in *Figure 2* and *Figure 3* is that when ε and $\eta \to 0$ the error norms of the consistent-capacitance FEM solutions using linear and homographic approximation do not approach to the same limits. As one can see from *Figure 3a* that the accuracy of temperature at small η and near the optimum η by the homographic approximation is much better than that at small ε and near the optimum ε by the linear approximation; and this accuracy improvement becomes more significant with mesh refinement. In *Figure 3b* the improvement of accuracy of flux by using homographic approximation is similar to the case for temperature, except for the first mesh. From *Figure 3c* we can see that for the whole range of ε and η and all the three meshes we tested, the homographic approximation predicts the interface position more accurately then does the linear approximation.

Our test results also indicate that the homographic approximation can help to improve the convergence behaviour of the consistent FEM solutions. For instance, at $\varepsilon = 10^{-4}$ the FEM flux solutions using linear approximation have a non-monotonic convergence tendency as shown in *Figure 3b*, where the $|e_2|$ of mesh 2 is worse than that of mesh 1. While the $|e_2|$ given by the homographic approximation shows monotonic convergence with a faster convergence rate at $\eta = 10^{-4}$. Another convergence improvement by using homographic approximation is observed for the low Stefan number cases. For example, when $L = 10$ (i.e. $St = 0.1$) we cannot obtain convergent FEM solutions from linear approximation via the Gauss–Seidel SOR iteration

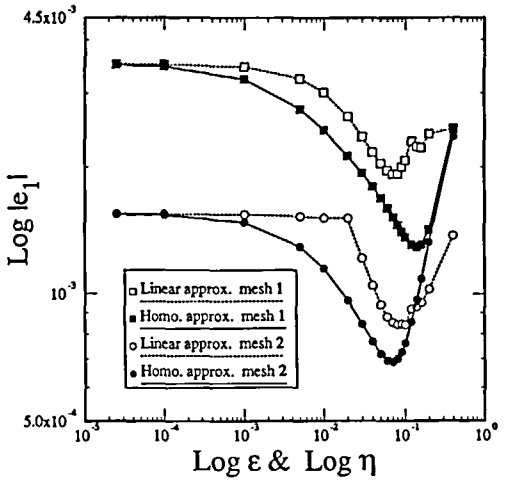

Figure 2 Effect of the parameters ε and η on the accuracy of the FDM (or equivalently the lumped-capacitance FEM) solutions based on the basic enthalpy formulation (4) for the test problem. The implicit backward scheme, by setting $\theta = 1$ in (7), is used with $\Delta t = \Delta x = 0.1$ for mesh 1 and $\Delta t = \Delta x = 0.05$ for mesh 2. The accuracy of temperature is measured by the global error norm $|e_1|$ defined in (39)

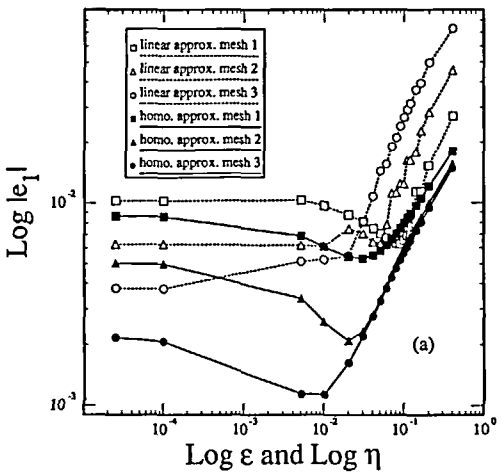

Figure 3a The temperature error norm $|e_1|$ (39)

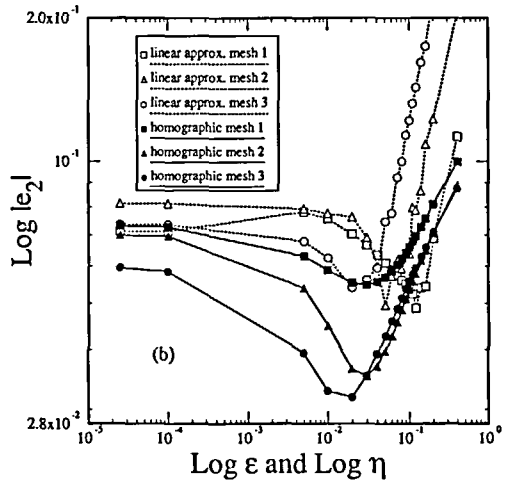

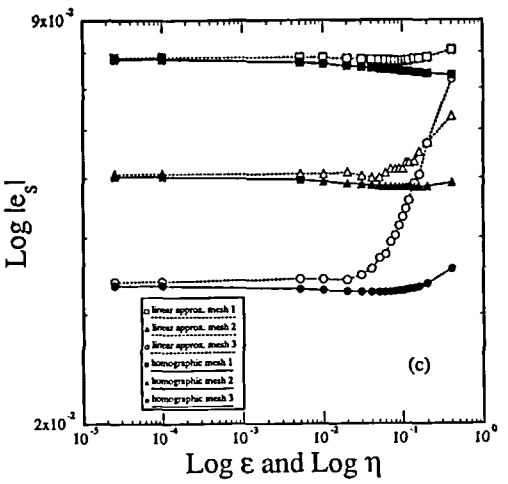

Figure 3 Accuracy and convergence improvement by using homographic approximation for the consistent-capacitance FEM solutions based on the basic enthalpy formulation (4) for the test problem. The Crank–Nicholson scheme, by setting $\theta = 0.5$ in (8), is used with $\Delta t = \Delta x = 0.1, 0.05, 0.025$ for mesh 1, 2, 3, respectively; (b) the heat flux error norm $|e_2|$ (40); (c) the interface position error norm $|e_s|$ (41)

scheme, whereas the homographic approximation poses no problem at all for the non-linear iteration convergence.

Apparent heat capacity formulation

To test the homographic approximation for AHC formulation, we consider the lumped-capacitance FEM backward scheme (or equivalently the backward FDM scheme) by setting

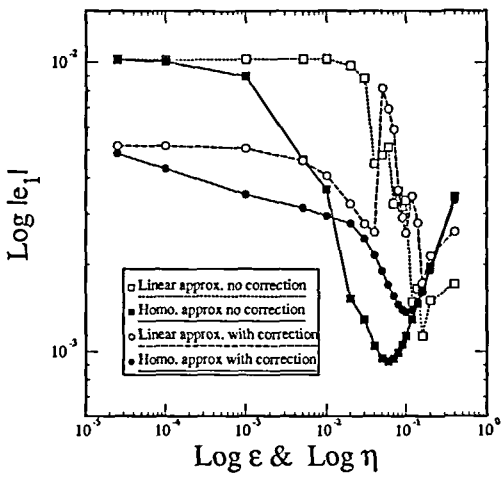

Figure 4 Comparison of solutions for the apparent heat capacity formulation. Two AHC expressions, i.e. (21) and (27) which correspond to the linear and homographic approximation respectively, are used. The backward scheme, by setting $\theta = 1$ in (11), is employed with $\Delta x = 0.1$ and $\Delta t = 0.05$. The post-iteration correction is performed using (12) and (13)

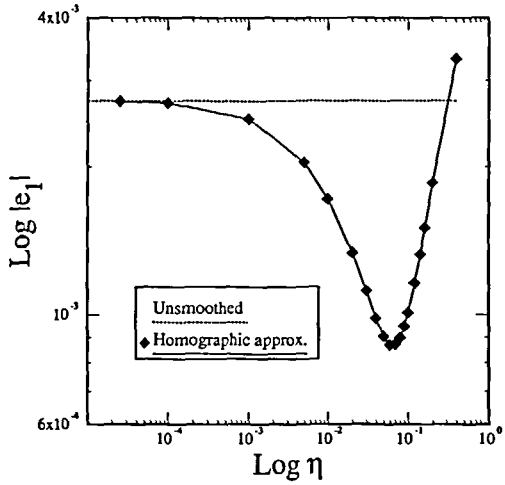

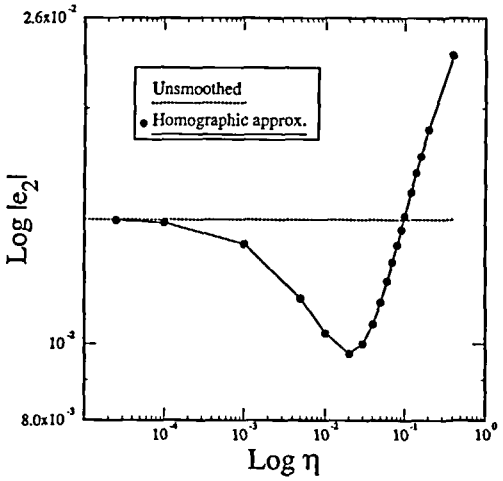

Figure 5 Comparison of the lumped-capacitance FEM (or equivalently the FDM) solutions in terms of $|e_1|$ and $|e_2|$ for the source term formulation. The implicit backward scheme is used with $\Delta x = 0.1$ and $\Delta t = 0.05$. The unsmoothed solution is based on formulation (17) and (6) and the homographic approximation solution is obtained using (36)–(38) and (22)

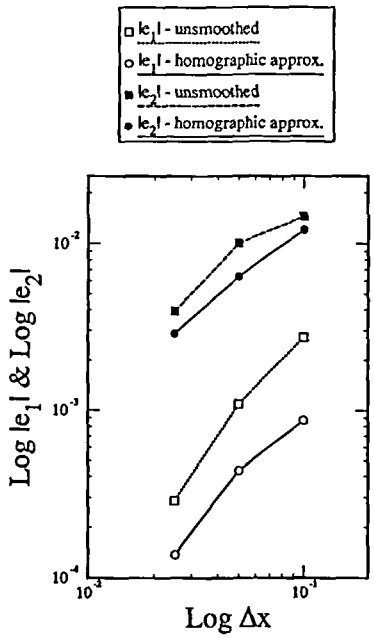

Figure 6 Convergence check with mesh refinement for solutions of the test problem. The formulations used are the same as in *Figure 5*. The implicit backward scheme is used with $\lambda = \Delta t/(\Delta x)^2 = 5$, $\Delta x = 0.1, 0.05, 0.025$ for meshes 1, 2, 3, respectively. The approximated optimum values of η employed in our computation are 0.06, 0.03, 0.01 for meshes 1 to 3, respectively

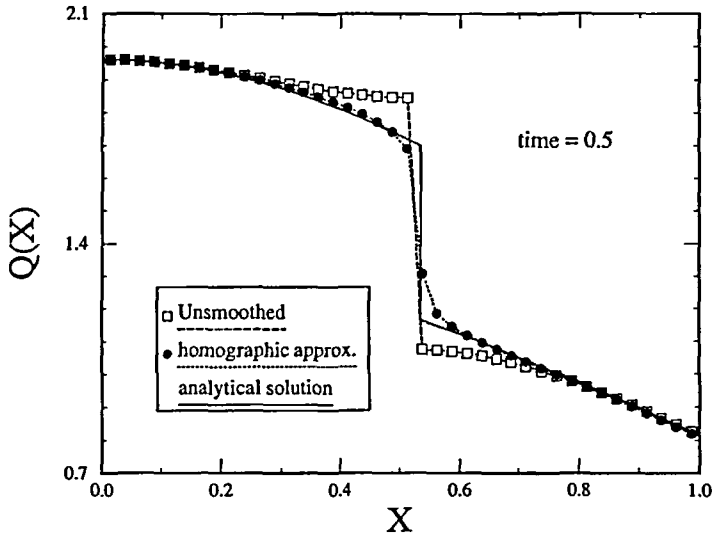

Figure 7 Plot of heat flux *versus* x at $t = 0.5$ sec for the test problem. The solutions shown are computed by the source term formulation (17) using the unsmoothed liquid fraction (6) and by the formulation (36) with the homographic approximation (22). The backward time integration scheme is used with $\Delta x = 0.025$, $\Delta t = 0.003125$ and $\eta = 0.005$. The unsmoothed liquid fraction tends to over-release the latent heat while the homographic approximation gives more accurate solution

$\theta = 1$ in (11). The AHC is approximated by the step function (21) and the corresponding homographic approximation (27). Both the solutions with and without the post-iteration correction are computed and some typical results are presented in *Figure 4*. The error norms shown in *Figure 4* indicate that homographic approximation can always help to improve the accuracy of temperature solution whether the post-iteration correction is used. Furthermore, for the conventional AHC method, i.e. when no post-iteration correction is applied, the accuracy improvement by the homographic approximation is more significant. It is interesting to note that for the two-level scheme we tested and based on the $|e_1|$ norm, the post-iteration correction only works for small values of ε and η ($\varepsilon \leqslant 0.05$ in linear approximation and $\eta \leqslant 0.01$ in homographic approximation as one can see from *Figure 4*). When ε and η are large, the post-iteration correction gives no accuracy improvement.

Source term formulation

To study the performance of homographic approximation in STF, we compute two sets of lumped-capacitance FEM solutions by the implicit backward scheme, the first set is obtained using the unsmoothed liquid fraction (6) and the formulation given in (17). The second set is based on the homographic approximation (22) and the formulation (36)–(38). In *Figures 5* and *6* we compare the two sets of solutions in terms of global error norms. The results presented in *Figure 5* again suggest the existence of the optimum values of η in homographic approximation. Note that the optimum values of η based on $|e_1|$ and $|e_2|$ may be different. When $\eta \to 0$ the accuracy of the two sets of solutions becomes the same. For a wide range of η (e.g. $10^{-4} < \eta < 10^{-1}$ for our test problem) the homographic approximation gives more accurate solutions and the accuracy improvement is much more significant near the optimal η. The convergence of the two sets of solutions with mesh refinement is shown in *Figure 6*.

For the STF, the homographic approximation can also help to improve the accuracy of temperature gradient near the solid/liquid interface. As a typical example, *Figure 7* shows that by using the unsmoothed liquid fraction the solution of heat flux is usually unsatisfactory in the neighbourhood containing the interface, whereas more accurate solution can be obtained by using the homographic approximation.

CONCLUSIONS

For the three typical numerical schemes of the enthalpy method tested in this paper, our numerical results show promising prospect for the application of the homographic approximation in phase change problems. Based on our numerical observations, the main features of the homographic approximation may be summarized as follows.

First and perhaps the most important, the approximated enthalpy function becomes C^1-continuous. Consequently, the definitions of enthalpy H_η, apparent heat capacity C_η^A and liquid fraction g_η are valid on the whole temperature range ($-\infty < T < +\infty$), in contrast to the case of linear approximation in which the definitions of the corresponding quantities, H_ε, C_ε^A and g_ε, have to be given piecewise on each of the three temperature intervals. Because of its simple definition, the homographic approximation is simple in formulation and easy to program.

Second, from the time integration point of view, the advantage of using homographic approximation is more distinct for implicit time integration schemes, especially when large time steps are used.

Third, from the numerical formulation point of view, due to the distributed nature of the capacitance matrix, the consistent-capacitance FEM formulation is more sensitive to the smoothness of the enthalpy function than the lumped-capacitance treatment. Therefore, the consistent FEM solutions can benefit the most from the homographic approximation. For a wide range of η-value (e.g. $\eta \leqslant \eta_0$, η_0 > optimum η) the homographic approximation results in more accurate solutions than the linear approximation in terms of the global error measurement. Furthermore, the accuracy and convergence improvement for the consistent FEM solutions by using the homographic approximation are much more significant than that in the FDM and the lumped-capacitance FEM. At low Stefan number the homographic approximation can also help to improve the convergence of non-linear iteration when the solutions using the linear approximation fail to converge.

Fourth, in the lumped-capacitance FEM and the FDM formulations, the homographic approximation can also help to improve the solution accuracy within a certain range of η-value. This improvement becomes more dramatic near the optimum η. Unfortunately, the optimum η is usually unknown beforehand and has to be determined through numerical experiment.

Last, pertaining to the application of the homographic approximation, an important difference between the lumped-capacitance FEM (or equivalently the FDM) and the consistent-capacitance FEM solutions is the behaviour of error norms at small values of ε and η. For the lumped-capacitance FEM solutions, the error norms obtained using unsmoothed, linear and homographic approximations approach to the same limits when $\varepsilon, \eta \to 0$. In contrast, for the consistent-capacitance FEM solutions, the error norms obtained by different smoothing schemes are generally different at small values of ε and η and the homographic approximation always gives better results. Therefore the homographic approximation is highly recommended for the consistent-capacitance FEM formulation.

Since there is no spatial variable involved in the $H-T$ relation, the application of homographic approximation to multidimensional phase change problems should be straightforward and similar

advantages as in 1-D case are expected. However, further work still needs to be done to evaluate the full benefits of using homographic approximation for the multidimensional problems.

In this work the homographic approximation has only been used for approximating the enthalpy function. It is worthy of mention that the homographic approximation can also be employed to approximate other functions with jump discontinuity, such as discontinuous material properties. For example, a piecewise constant heat conductivity can be approximated by:

$$\kappa(T) = \kappa_1 + \frac{(\kappa_2 - \kappa_1)}{2}\left(\frac{T - T_m}{\eta + |T - T_m|} + 1\right)$$

ACKNOWLEDGEMENTS

The authors would like to thank T. K. Glasgow of NASA Lewis Research Center and the other two anonymous referees for their valuable comments and useful input to this paper. This work is sponsored by the NASA's Microgravity Science and Application Program.

REFERENCES

1 Crank, J. *Free and Moving Boundary Problems*, Clarendon Press, Oxford (1984)
2 Shamsundar, N. Comparison of numerical methods for diffusion problems with moving boundaries, in *Moving Boundary Problems*, (Eds D. G. Wilson and P. T. Boggs), Academic Press, New York, pp. 165–185 (1978)
3 Furzeland, R. M. A comparative study of numerical methods for moving boundary problems, *J. Inst. Maths Applns*, 26, 411–429 (1980)
4 Poirier, D. and Salcudean, M. On numerical methods used in mathematical modeling of phase change in liquid metals, *J. Heat Transfer Trans. ASME* 110, 564–570 (1988)
5 Lewis, R. W. and Roberts, P. M. Finite element simulation of solidification problems, *Appl. Scient. Res.* 44, 61–92 (1987)
6 Dantzig, J. A. Modeling liquid–solid phase changes with melt convection, *Int. J. Num. Meth. Eng.* 28, 1769–1785 (1989)
7 Voller, V. R. and Swaminathan, C. R. Fixed grid techniques for phase change problems: a review, *Int. J. Num. Meth. Eng.* 30, 875–898 (1990)
8 Voller, V. R. Some comments on: benchmark problems and testing of a finite element code for solidification in investment castings, *Int. J. Num. Meth. Eng.* 33, 213–216 (1992)
9 Tamma, K. K. and Namburu, R. R. Recent advances, trends and new perspectives via enthalpy-based finite element formulations for applications to solidification problems, *Int. J. Num. Meth. Eng.* 30, 803–820 (1990)
10 Voller, V. R. and Swaminathan, C. R. General source-based method for solidification phase change, *Num. Heat Transfer*, (*B*) 19, 175–189 (1991)
11 White, R. E. *An Introduction to the Finite Element Method with Applications to Nonlinear Problems*, John Wiley, New York (1985)
12 Budak, B. M., Sobol'eva, E. N. and Uspenskii, A. B. A difference method with coefficient smoothing for the solution of Stefan problems, *USSR Comput. Math. Math. Phys.* 5, 59–75 (1965)
13 Ladyzenskaja, O. A., Solonnikov, V. A. and Ural'ceva, N. N. Linear and quasi-linear equations of parabolic type, *AMS Transl.*, Providence, Rhode Island, 23, 449 (1968)
14 Crowley, A. B. On the weak solution of moving boundary problems, *J. Inst. Maths. Appln* 24, 43–57 (1979)
15 Tacke, K. Discretization of the explicit enthalpy method for planar phase change, *J. Num. Meth. Eng.* 21, 543–554 (1985)
16 Goodrich, L. E. Efficient numerical technique for one-dimensional thermal problems with phase change, *Int. J. Heat Mass Transfer* 21, 615–621 (1978)
17 Voller, V. and Cross, M. Accurate solutions of moving boundary problems using the enthalpy method, *Int. J. Heat Mass Transfer* 24, 545–556 (1981)
18 Brauner, C. M., Frémond, M. and Nicolaenko, B. A new homographic approximation to multiphase Stefan problems, in *Free Boundary Problems: Theory and Applications*, (Eds A. Fasano and M. Primicerio), Elsevier, Amsterdam, pp. 365–379 (1982)
19 Blanchard, D. and Frémond, M. The Stefan problem: computing without the free boundary, *Int. J. Num. Meth. Eng.* 20, 757–771 (1984)
20 Luikov, A. V. *Analytical Heat Diffusion Theory*, Academic Press, New York (1968)

21 Voller, V. R. Fast implicit finite-difference methods for the analysis of phase change problems, *Num. Heat Transfer, (B)* **17**, 155–169 (1990)
22 Cook, R. D., Malkus, D. S. and Plesha, M. E. *Concepts and Applications of Finite Element Analysis*, 3rd Edn, John Wiley, New York (1989)
23 Pham, Q. T. The use of lumped capacitance in the finite-element solution of heat conduction problems with phase change, *Int. J. Heat Mass Transfer* **29**, 285–291 (1986)
24 Dalhuijsen, A. J. and Segal, A. Comparison of finite element techniques for solidification problems, *Int. J. Num. Meth. Eng.* **23**, 1807–1829 (1986)
25 Hashemi, H. T. and Sliepcevich, C. M. A numerical method for solving two-dimensional problems of heat conduction with change of phase, *Chem. Eng. Progr. Symp. Series*, **63**, 34–41 (1967)
26 Comini, G., Del Guidice, S., Lewis, R. W. and Zienkiewicz, O. C. Finite element solution of non-linear heat conduction problems with special reference to phase change, *Int. J. Num. Meth. Eng.* **8**, 613–624 (1974)
27 Comini, G., Del Giudice, S. and Saro, O. A conservative algorithm for multidimensional conduction phase change, *Int. J. Num. Meth. Eng.* **30**, 697–709 (1990)
28 Bonacina, C., Comini, G., Fasano, A. and Primicerio, M. Numerical solution of phase-change problems, *Int. J. Heat Mass Transfer*, **16**, 1825–1832 (1973)
29 Brauner, C. M. and Nicolaenko, B. On nonlinear eigenvalue problems which extend into free boundaries problems, in *Proc. Conf. Nonlinear Eigenvalue Problems, (Lect. Notes in Math. 782)*, Springer-Verlag, Berlin, pp. 61–100 (1979)
30 Brauner, C. M. and Nicolaenko, B. Free boundary value problems as singular limits of nonlinear eigenvalue problems, in *Proc. Symp. Free Boundary Problems*, (Ed. E. Magenes Pavia), Istituto Nazionale di Alta Mathematics Francesco Severi (Roma) Publisher, Vol. II, 61 (1980)
31 Brauner, C. M. and Nicolaenko, B. Singular perturbations and free boundary value problems, in *Proc. 4th Int. Symp. Comp. Meth. Appl. Sci. Eng.*, North Holland, Amsterdam, pp. 699–724 (1980)
32 Stefan, J. *Ann. Phys. U. Chem., (Wiedemann)* (N.F.) **42**, 269–286 (1891)
33 Elliott, C. *DPhil Thesis*, Oxford University (1976)
34 Voller, V. R., Cross, M. and Walton, P. Assessment of weak solution techniques for solving Stefan problems, in *Numerical Methods in Thermal Problems* (Eds R. W. Lewis and K. Morgan), Pineridge Press, Swansea, p. 172 (1979)
35 Yao, M. and Chait, A. A numerical study of the enthalpy method, in preparation